

# Multiple wavelength heterodyne array interferometry

Lenore McMackin and David G. Voelz

Advanced Optics and Imaging Division, Air Force Research Laboratory  
3550 Aberdeen Ave SE  
Kirtland AFB, NM 87117-5776

mcmackin@plk.af.mil

Matthew P. Fetrow

Applied Technology Assoc.'s, 1900 Randolph SE, Albuquerque, NM 87106

**Abstract:** Multiple wavelength interferometry is combined with a heterodyne array sensing technique to provide an approach for measuring highly aberrated optical surfaces. Interferometric measurements created with long effective wavelengths are obtained by digitally combining complex exposures collected at different optical wavelengths. The heterodyne array sensing method is straightforward to implement and holds promise for rapid wavefront measurements with high spatial and phase resolution. Measurements of a tilted, flat surface are presented and analyzed.

©1997 Optical Society of America

OCIS code: (120.3180) Interferometry; (040.2840) Heterodyne

---

## References and Links

1. D. K. Marker and C. H. Jenkins, "Surface precision of optical membranes with curvature," *Opt. Express* **1**, 324-331 (1997).  
<http://epubs.osa.org/oearchive/source/2668.htm>
2. *Holographic Interferometry*, P.K. Rastogi, ed., Springer Ser. Opt. Sci. **68**, (Springer, Berlin, 1994).
3. P. Hariharan, "Quasi-heterodyne hologram interferometry," *Opt. Eng.* **24**, 632-638 (1985).
4. Y. Ishii, J. Chen, and K. Murata, "Digital phase-measuring interferometry with a tunable laser diode," *Opt. Lett.* **12**, 233-235 (1987).
5. I. Yamaguchi, J. Liu, and J. Kato, "Active phase-shifting interferometers for shape and deformation measurements," *Opt. Eng.* **35**, 2930-2937 (1996).
6. D. G. Voelz, L. McMackin, J. K. Boger, and M. P. Fetrow, "Double-exposure heterodyne imaging for observing line-of-sight deformation," *Opt. Lett.* **22**, 1027-1029 (1997).
7. J. C. Wyant, "Testing aspherics using two-wavelength holography," *Appl. Opt.* **10**, 2113-2118 (1971).
8. K. Creath, "Step height measurement using two-wavelength phase-shifting interferometry," *Appl. Opt.* **26**, 2810-2816 (1987).
9. R. Dandliker, R. Thalmann and D. Prongue, "Two-wavelength laser interferometry using superheterodyne detection," *Opt. Lett.* **13**, 339-341 (1988).
10. E. Gelmini, U. Minoni, and F. Docchio, "Tunable, double wavelength heterodyne detection interferometer for absolute distance measurements," *Opt. Lett.* **19**, 213-215 (1994).

---

## 1. Introduction

The use of large, light-weight, optical elements is essential for applications that require large collecting areas but have cost or weight restrictions. One technology under consideration for this purpose is membrane optical elements.<sup>1</sup> For elements of this type to be viable, methods for optically measuring highly aberrated surface structures will need to be employed - not only for characterization purposes, but possibly for real-time figure and surface control. Such an optical profiling system may need to provide a spatial resolution of several thousand points

and will have to deal with aberrations ranging from hundreds of optical waves to a fraction of a wave. In addition, a useful profilometer system will need to be compact, light-weight, rugged, and capable of a measurement time, or frame rate, that can approach "real-time".

In this paper we describe a surface profiling approach that addresses the above requirements. The fundamentals of the approach are common to those of electro-optic holography.<sup>2</sup> However, we have introduced a digitally-based, two-wavelength measurement scheme to provide the interferometer with a variable sensitivity capability. Our sensing approach employs a heterodyne phase measurement at each pixel in a CCD array where the resulting two-dimensional map of phase values is related to the optical path length profile of the surface under examination. This approach for surface measurement was presented by Hariharan<sup>3</sup> as "quasi-heterodyne hologram interferometry". In that work and most subsequent efforts<sup>4,5</sup> discrete phase-stepping techniques were implemented to obtain the phase measurements. We use a continuous phase-shift approach that is accomplished using acousto-optic modulators (AOMs).<sup>6</sup> Phase measurements are obtained by interfering an object and reference beam of slightly different frequencies. The resulting temporal beat signal is sampled at each point in the interference pattern so that the phase can be calculated. The AOMs and associated drive circuitry can provide stable frequency shifts as small as a few Hertz, which allows the use of an off-the-self CCD camera as the sensing element. In general, we have found the AOM-based system to be very reliable and robust (containing no moving parts), and simple to implement.

When hundreds of optical waves of aberration are present conventional interferometric measurement at visible wavelengths produces too many fringes to count. Historically, methods for optical testing in such cases have combined interferograms or holograms that were created at two different wavelengths.<sup>7-10</sup> The range of optical path length that can be measured is increased using two-wavelength techniques that create a synthetic wavelength much longer than the optical regime. Measurement sensitivity is proportional to this equivalent wavelength rather than the optical wavelength.

In our system a heterodyne array measurement is made for each of two different probe laser wavelengths and each frame is stored in the computer in complex exponential form. These digital phase frames are then differenced in the computer to produce optical path length maps that are associated with different synthetic wavelengths. A single tunable laser is employed that can be scanned quickly in wavelength, which provides for nearly continuously variable-sensitivity phase measurements from which large and small surface deviations on the same surface can be defined. As an additional note, the advantage of working with the phase frames in a complex exponential form in the computer is that differencing of frames, or other multi-frame operations, can be performed without concern about  $2\pi$  phase jumps since all operations are carried out modulo- $2\pi$ . Phase unwrapping is performed only on the final result frame.

The digital super-heterodyne interferometry technique described here owes its utility and affordability to recent advances in laser devices, CCD cameras and computer technology. Tunable diode lasers can provide great flexibility for generating different synthetic wavelengths. Data rates required for real-time applications can be obtained with off-the-shelf high frame-rate CCD cameras. Frame grabbers and PC-based computer systems now have enough memory and processing speed to handle the data acquisition rates and phase computations required for a timely measurement.

## 2. Theory

The heterodyne sensing part of our concept has been described previously for an imaging system that measures line-of-sight deformation.<sup>6</sup> In summary, a coherent probe beam is reflected from a test surface and combined with a reference beam on a CCD camera. The probe and reference beams have slightly different optical frequencies and the resulting temporally beating intensity signal on the CCD camera is sampled and stored for each pixel. A phase

value is computed for each pixel using a simple Fourier coefficient-based algorithm. Amplitude values at each pixel are combined with the phase information and a complex exposure is formed in the computer. A complex exposure is given by

$$E_a(\mathbf{r}_m, \lambda_a) = A_a(\mathbf{r}_m, \lambda_a) \exp\{j(\phi_a(\mathbf{r}_m, \lambda_a) + \phi_{\text{ref}a})\}, \quad (1)$$

where  $\mathbf{r}_m$  is a two dimensional pixel location,  $\lambda_a$  is the illuminating wavelength,  $A_a(\mathbf{r}_m, \lambda_a)$  is the product of the amplitudes of the image and reference wavefronts,  $\phi_a(\mathbf{r}_m, \lambda_a)$  is the phase of the test wavefront and  $\phi_{\text{ref}a}$  is the constant phase of the reference wavefront. The exposure has been purposely represented in a complex exponential form because differencing or summing of different exposures can now be done modulo- $2\pi$  so that  $2\pi$  phase jumps are not a concern.

Now consider a second complex exposure measured using the illumination wavelength,  $\lambda_b$ . This exposure is described by

$$E_b(\mathbf{r}_m, \lambda_b) = A_b(\mathbf{r}_m, \lambda_b) \exp\{j(\phi_b(\mathbf{r}_m, \lambda_b) + \phi_{\text{ref}b})\}. \quad (2)$$

In typical applications, the difference between  $\lambda_a$  and  $\lambda_b$  may be just a few nanometers so  $A_a$  and  $A_b$  are essentially equivalent but the phase values can be quite different. By evaluating the following quantity in the computer, we can find the difference between the two image phase functions,

$$\arg\{E_a(\mathbf{r}_m, \lambda_a)E_b(\mathbf{r}_m, \lambda_b)^*\} = \phi_a(\mathbf{r}_m, \lambda_a) - \phi_b(\mathbf{r}_m, \lambda_b) + \phi_{\text{ref}a} - \phi_{\text{ref}b}. \quad (3)$$

In practice, a synchronization of the heterodyne data collection process can be arranged so the two constant terms  $\phi_{\text{ref}a}$  and  $\phi_{\text{ref}b}$  are equal and thus cancel. Similarly, it is straightforward to remove a constant value from the result in Eq. (3). Deleting these terms leaves an "equivalent" phase that is related to the optical path difference (OPD) between the surface of the object and the flat reference wavefronts,<sup>8</sup>

$$\phi_{\text{eq}}(\mathbf{r}_m, \lambda_a) = \phi_a(\mathbf{r}_m, \lambda_a) - \phi_b(\mathbf{r}_m, \lambda_b) = 2\pi\text{OPD}(\mathbf{r}_m)/\lambda_{\text{eq}}, \quad (4)$$

where

$$\lambda_{\text{eq}} = \lambda_a\lambda_b / |\lambda_a - \lambda_b|. \quad (5)$$

So the result in Eq. (4) is equivalent to that of a single interferometric measurement of the test surface using the wavelength,  $\lambda_{\text{eq}}$ .

### 3. Experimental setup and results

The heterodyne interferometer setup is shown in Fig. 1. The illumination source is a diode laser that nominally operates at a wavelength of 780 nm and is tunable over a 20-nm range with steps as fine as 0.1 nm. After passing through some attenuation optics, the beam is split into a probe leg and a reference leg. An acousto-optic modulator (AOM) in each leg shifts the frequency of the beams by 40 MHz with an additional 8-Hz shift being applied to the probe beam. Both beams are expanded and the probe beam continues on to the test surface while the reference beam is sent to the camera face. Reflected light from the test surface is returned to the camera face where it interferes with the reference beam producing an 8-Hz modulated intensity signal. A standard video rate (30 Hz) camera and frame grabber/Pentium PC system captures 16 consecutive intensity frames from which the 8-Hz signal is demodulated for each pixel and a complex exposure is produced (Eq. (1)). Complex exposures

at different wavelengths are obtained by tuning the diode laser to different lines and collecting and processing accompanying sets of intensity frames. Although not shown in Fig. 1, it is possible to include optics in front of the camera to form an image of the test surface or some other object at the camera face.

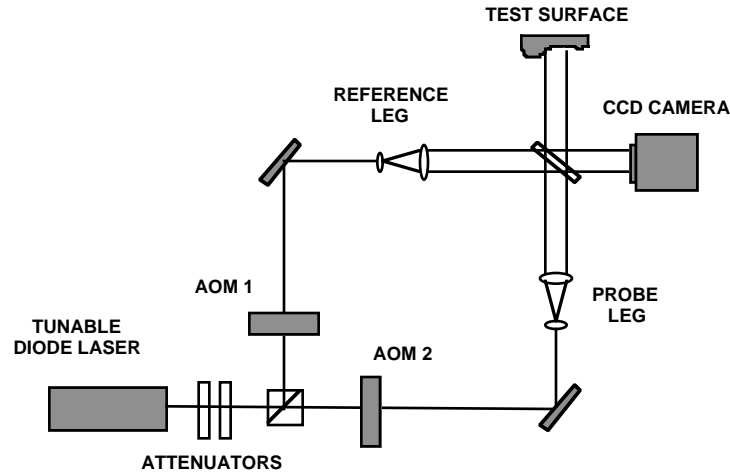


Figure 1. Diagram of heterodyne array profilometer.

To test the system in the laboratory a tilted flat mirror was examined. A portion of the mirror, approximately 6-mm square, was observed by the system and the mirror wavefront was tilted with respect to the reference wavefront by about  $70 \mu\text{m}/\text{mm}$ . This fixed surface was measured using 7 different synthetic wavelengths generated from combinations of pairs of complex exposures (Table 1). A sequence of the seven equivalent wavelength phase maps produced in the lab is shown in Fig. 2. As the equivalent wavelength increases the number of  $2\pi$  phase jumps across the surface decreases. This is expected since the tilt of the mirror wavefront is being recorded as phase values relative to the effective wavelength. In Fig. 3 the  $2\pi$  phase jumps have been removed using a simple phase-unwrapping routine and the phase profiles are presented as a series of surface plots. The surface profiles show less and less slant as the equivalent wavelength increases. In essence, the longer the effective wavelength the less sensitive the measurement is to optical path length or depth. It is this feature that allows optical paths of many hundreds of optical wavelengths to be measured without counting hundreds of fringes. In Fig. 4 the phase profile results have been scaled by the effective wavelength to yield absolute optical path length in micrometers. In this case the slant of the measured profile is constant at the different effective wavelengths, which shows the mirror wavefront is not changing tilt between measurements. As expected, the absolute measurement noise increases as the effective wavelength increases.<sup>2</sup>

An estimate of the fidelity of the heterodyne array phase measurement for our setup was made by comparing two consecutive phase profiles collected with the same wavelength (optical or effective). The phase values for the two frames were differenced, pixel-by-pixel, and then the standard deviation of this error over the  $640 \times 480$  pixels was calculated. For the single optical wavelength measurement this standard deviation was typically about  $\lambda/120$ . For the effective wavelength measurements the standard deviation ranged from about  $\lambda_{\text{eq}}/60$  for  $\lambda_{\text{eq}}=40 \mu\text{m}$  to  $\lambda_{\text{eq}}/70$  for  $\lambda_{\text{eq}}=600 \mu\text{m}$ .

Table 1. Complex exposure wavelengths and resulting equivalent wavelengths

$\lambda_a$ ( $\mu\text{m}$ )	$\lambda_b$ ( $\mu\text{m}$ )	$\lambda_{eq}$ ( $\mu\text{m}$ )
0.792	0.7766	40
0.792	0.7817	60
0.792	0.7842	80
0.792	0.7858	100
0.792	0.7889	200
0.792	0.7910	600
0.792	0.7912	800

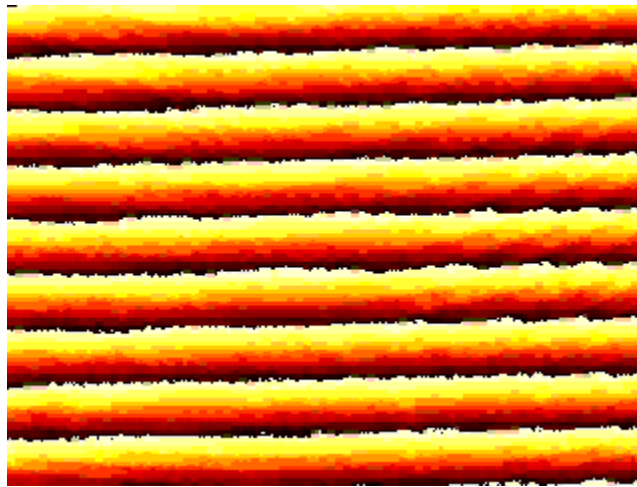


Figure 2. Phase maps of a tilted surface for the equivalent wavelengths in Table 1.

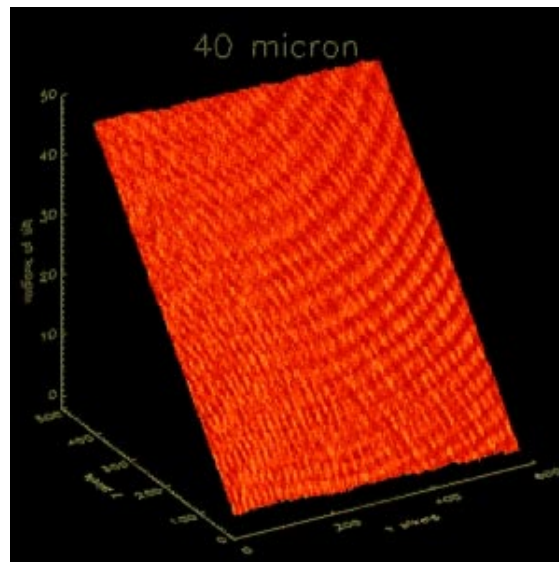


Figure 3. Unwrapped phase profile plots of a tilted surface for the equivalent wavelengths in Table 1.

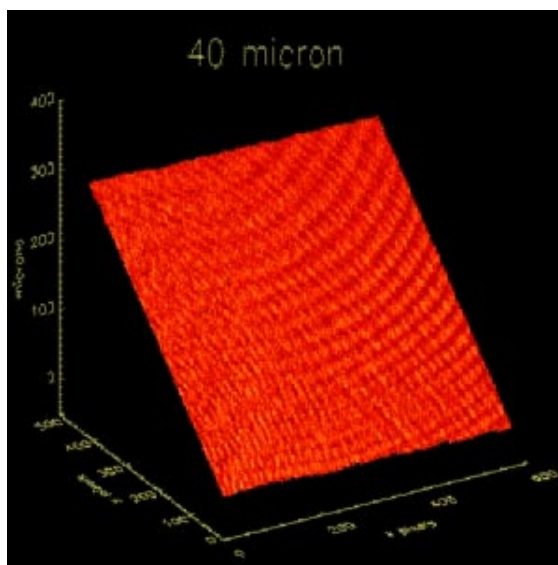


Figure 4. Optical path profiles of a tilted surface for the equivalent wavelengths in Table 1.

#### 4. Summary

The multiple wavelength heterodyne array profilometer described and demonstrated here has the following strengths: 1) the use of multiple wavelengths generated by a diode laser provides for a large and variable range of optical path length measurement, 2) the heterodyne phase sensing approach is easily implemented with simple, compact and reliable hardware, and 3) wavefronts can be measured with high phase resolution as well as high, two-dimensional, spatial resolution. These attributes make this wavefront sensing approach attractive for measuring the surface structure and wavefront quality of large, highly aberrated optics. The heterodyne array sensing approach holds promise for high-speed phase measurement without sacrificing spatial or phase resolution. This promise stems from the fact that the phase processing is inherently a parallel operation involving no cross-pixel calculations and is simple enough in principle to be implemented in a digital or analog fashion on a sensor chip. The possibility of rapid wavefront measurement makes this approach of interest for “real-time” control of adaptive optical systems.

In addition to the innovation of combining heterodyne array sensing with multiple wavelength measurements, we also employ the approach of working with the digital complex exposures in the computer in a complex exponential form. The differencing of complex exposure frames, or other multi-frame linear operations of interest, can be performed as complex exponentials without concern about  $2\pi$  phase jumps since all operations are carried out modulo- $2\pi$ .

#### Acknowledgments

The authors thank Laura Ulibarri, Mervyn Kellum, and Ken MacDonald for assisting with the laboratory measurements and data processing.